Chapter 9

Self-embedded nanocrystalline chromium carbides on well-aligned carbon nanotips

9.1. Introduction

Well-aligned carbon nanotips embedded with nanocrystalline chromium carbide were directly grown on a substrate by microwave plasma chemical vapor deposition. These nanomaterials grew up to about 1 μm long and 60 nm in diameter, yielding a high aspect ratio. In comparison between carbon nanotubes with hollow structure, transmission electron microscopy images show its solid body, which is made of graphite along with nanocrystalline chromium carbide on the tip. These nanomaterials perform well in field emission applications with a turn-on field of 1.38 V/μm and 565 μA/cm^2 at 2.2 V/μm. Our result confirms the possibility of the self-embedded of nanocrystalline materials on the top of carbon nanotips.

Carbon can bond in different ways to create structures with very different properties. Since the discovery of carbon nanotubes in 1991 [1], the synthesis of carbon-encapsulated composite nanostructure has attracted much attention. Experiments on nanotubes imply that they are suitable for use in many applications, such as scanning microscope probes [2] and electron field emitters [3-5]. The introduction of metals into multi-walled carbon nanotubes may significantly alter their

conducting, electronic and mechanical properties, as well as altering the properties of the metal.

This study describes nanocrystalline particles capped on the top of the carbon nanomaterials. The aim of this article is to contribute to the characterization of well-aligned carbon nanotips with embedded of nanocrystalline chromium carbides (CNTWNCCs). These nanocrystalline particles offer a confined space in which nanoscience can be conducted. Restated, these metal nanoparticles act as templates rather than catalysts. The presented results show the possibility of the self-embedded of nanoparticles on the top of the carbon nanotips.

9.2. Experiment
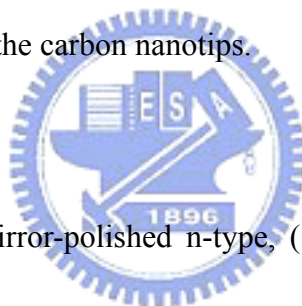
Starting substrates were mirror-polished n-type, (100) oriented Si wafers with a resistivity of 4.5~5.5 Ω/cm. Wafers were cleaned by RCA cleaning process to remove contamination on the silicon surface. After cleaning, a SiO_2 dielectric layer was deposited using a high-temperature and low-pressure furnace deposition system (model ASM LB-45). A 150 nm thick film of Cr was deposited on SiO_2 by using a dual E-Gun Evaporator (model ULVAC EBX-10C, Japan). Then, substrates underwent microwave plasma chemical vapor deposition (MPCVD) to grow CNTWNCCs. Before deposition, H_2 plasma treatment was used to activate the chromium films and to secondly clean the surface of the substrate. The reactive gases

used in deposition were CH_4/H_2 with the flow rate of 10/25 sccm. The growth

temperature; pressure and time were 800 ℃; 15 torr and 30 mins, respectively.

During deposition, a -120 V bias was applied to the samples.

After deposition, the produced CNTWNCCs were characterized using a scanning

electron microscope (SEM) to observe their length and morphology. High-resolution

transmission electron microscope (HRTEM) and energy dispersed X-ray spectrum

(EDX) were used to determine the nanostructure of individual CNTWNCCs and the

component of nanocrystalline materials. An I-V measuring system was used to obtain

the field emission property.

9.3. Results and Discussion

(I) Scanning electron microscope (SEM)

Figures 9.1 (a) and (b) show the cross-section and top view morphology of

CNTWNCCs. It is found that each uniform CNTWNCCs is significantly well-aligned

to the substrate. In addition, Figure 9.1 (c) clearly displays the nanocrystalline

chromium carbide on the top of the well-aligned carbon nanotips. Many studies about

aligned carbon nanotubes also have been reported elsewhere [6-8]. However,

high-magnification SEM pictures show that partial carbon nanotubes are not

well-aligned. Strictly speaking, this result implies that alignment is a macroscopic

property, not an individual phenomenon: a bundle of carbon nanotubes is aligned. The

alignment of carbon nanotubes is a result of Van der Walls interactions between neighboring nanotubes. Compared to the alignment of carbon nanotubes, it is speculated that the alignment of CNTWNCCs is primarily resulted from plasma-induced effect. This suggests that the CNTWNCCs orientation is influenced by the electrical field established on the immersed substrate surface in the plasma. Under such condition, the preferable orientation of CNTWNCCs is perpendicular to the substrate, causing them well-aligned. Certainly, applied a negative bias to result in a strong electrical field could enhance the alignment of CNTWNCCs.

Initially, H_2 plasma pre-treatment is used not only to clean the surface of the substrate, but also to activate the Cr film into nanoparticles on the substrate, offering a confined space for the growth of carbon nanotips. As growing carbon nanotips, the Cr nanoparticles are lifted off from the substrate and carburized into nanocrystalline chromium carbides. Our previous work have been explained the growth mechanism of carbon nanotips [9]. The final generation of Cr particles may be due to the interaction between Cr and the substrate. The growing carbon nanotips gradually lift off the Cr particles because of the weak force between Cr and the substrate. This growth mechanism is analogous to the tip-growth model of carbon nanotubes [10]. It is worth emphasizing that the optimum H_2 / CH_4 ratio for generating CNTWNCCs is 25/10 sccm. Once the ratio beyond 25/10 sccm, meaning the concentration of carbon is

increased, higher growth rate of the nanotips causes the coalescence of individual

nanotip to become continuous films. As the ratio exceeds 25/10 sccm, higher etching

rate resulted from the decomposed hydrogen leads to the Cr nanoparticles ambiguous

on the top of the tip. Based on SEM pictures, CNTWNCCs grow up to about 1 μm

long and 60 nm in diameter, causing them to exhibit a high aspect ratio, and making

them good candidates for the application of field emission.

(II) Transmission electron microscope (TEM)

Figure 9.2 (a) reveals the TEM images of CNTWNCCs. Nanocrystalline chromium

carbides are clearly embedded on the top of the carbon nanotips. Sparse carbon

nanotubes attached to the nanocrystalline chromium carbides are also observed. This

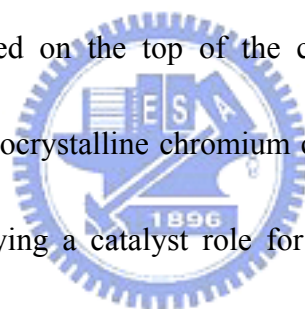is resulted from Cr film playing a catalyst role for the growth of nanotubes [11].

Figure 9.2 (b) shows the individual carbon nanotips with nanocrystalline chromium

carbide. Unlike hollow carbon nanotubes, Fig. 9.2 (c) shows that the carbon nanotips

have a solid structure. Our previous work provides further information about carbon

nanotips [9].

Figure 9.3 (a) shows a TEM image of an individual chromium carbide particle. The

high-resolution TEM image depicts nanocrystalline chromium carbide. The

diffraction pattern (DP) taken from the chromium carbide in Fig. 9.3 (b) also clearly

proves its nanocrystalline structure. Further analysis of chromium carbides is

performed by EDX technique. EDX spectrum shown in Fig. 9.4 (a) provides a direct

evidence of the chromium and carbon elements in chromium carbide.

Figure 9.4 (b) shows EELS spectra of the C K-edge and Cr L-edge obtained from

the individual nanocrystalline chromium carbide. It is found that the EELS spectrum

of carbon shows two components, i.e. the π line at 285 ev and σ line at 291 ev,

respectively. The π line and σ line are corresponding to the sp^2 and sp^3 of carbon

bonding. The oxygen and silicon peaks in the EELS spectrum are not observed. Thus,

it is definitely revealed that the nanoparticles consist of two elements; carbon and

chromium. The idea of possible compound of oxygen; carbon; silicon and chromium

can be ruled out. However, the specific compound of chromium carbides is not clear.

By calculating the lattice parameter of chromium carbides from diffraction pattern,

there is no related chromium carbide compounds. The ratio (5/3) of carbon to

chromium obtained from EELS is also not consistent with one of the chromium

carbide compounds. Besides, the carbon signal from EELS is not absolute amount

because of the noise coming from atmosphere or/and glue. This uncertain definition

of chromium carbides maybe due to the lattice defect and partial carburization.

(a)

1.38 μm
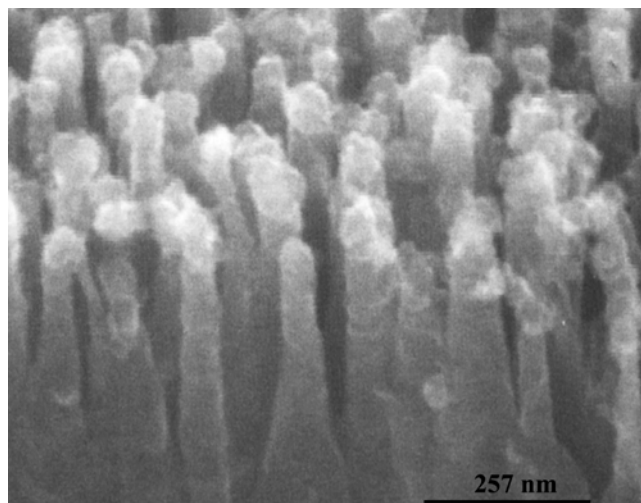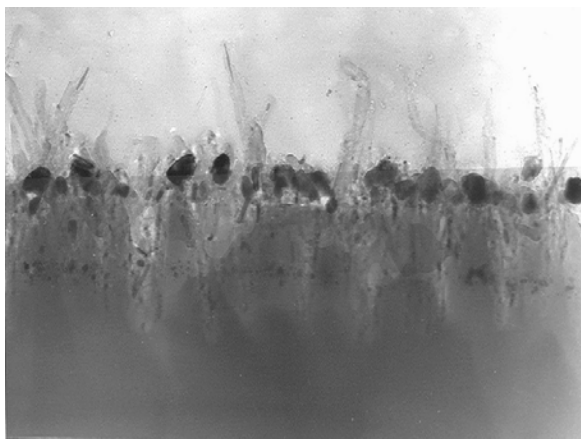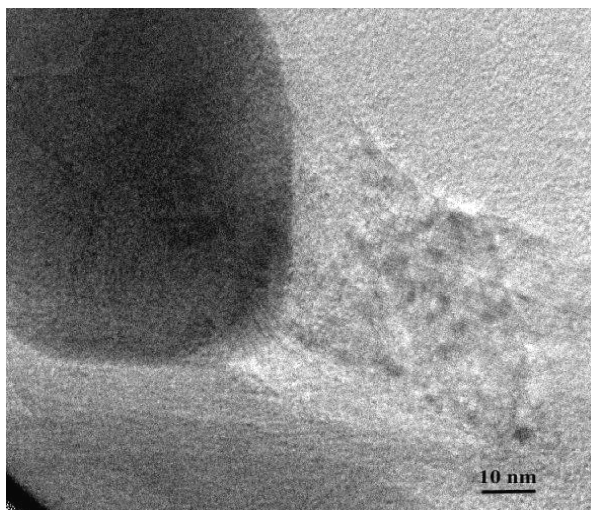
(b)

719 nm

(c)

257 nm
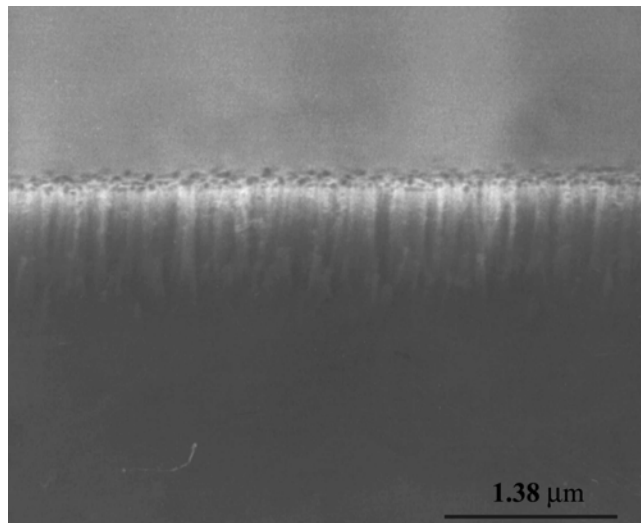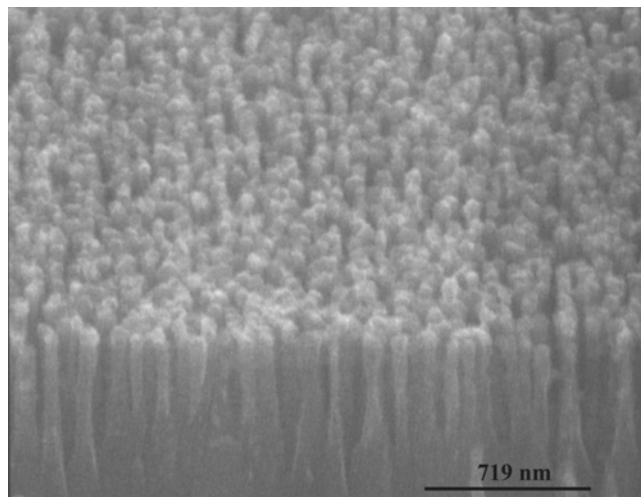
Fig. 9.1 SEM photographs of (a) cross-section view; (b) top view and (c) high magnification images of CNTWNCCs.
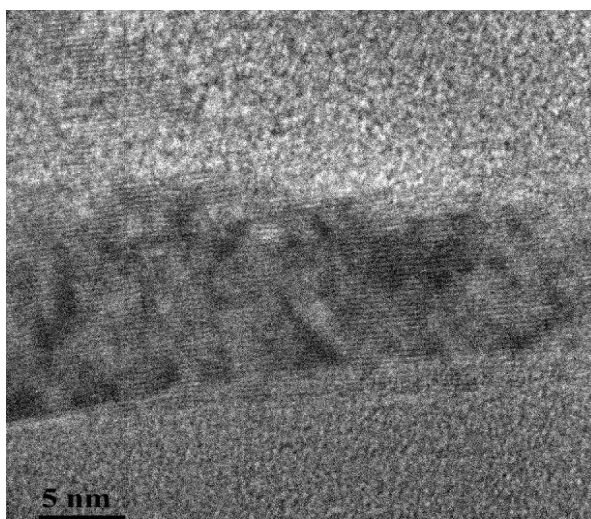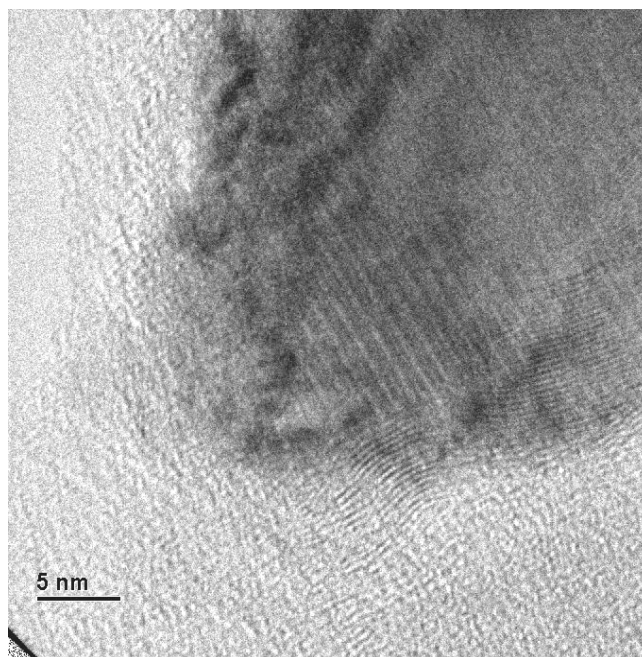
(a)

(b)

(c)

Fig. 9.2 TEM images of (a) cross-section view; (b) individual of CNTWNCCs and (c) the lateral section of carbon nanotip.
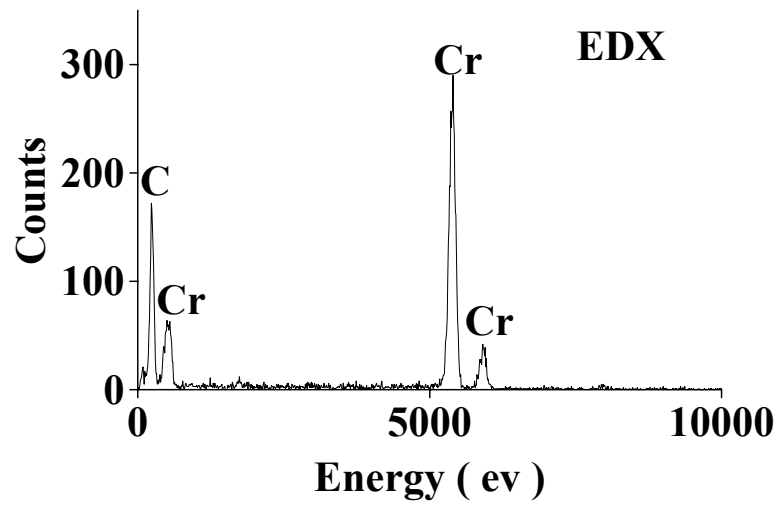
(a)

(b)

Fig. 9.3 (a) TEM images; and (b) diffraction pattern (DP) (c) EDX spectrum of

nanocrystalline chromium carbide, respectively.
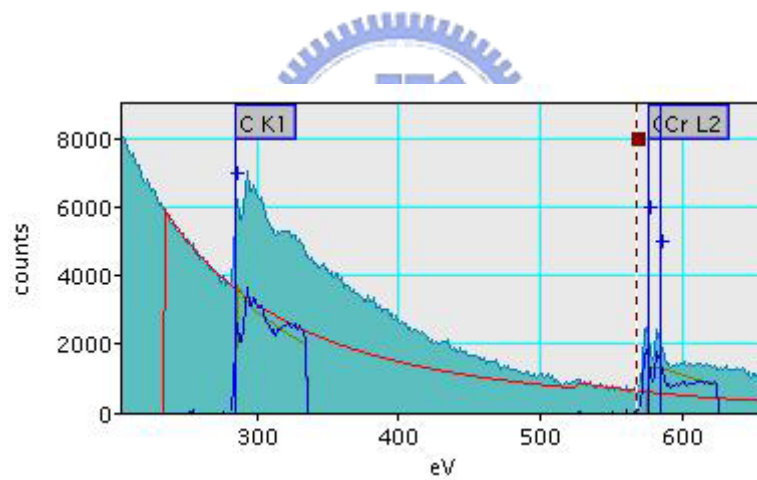
(a)

(b)

Fig. 9.4 (a) EDX and (b) EELS spectrum of nanocrystalline chromium carbide,

respectively.

(III) I-V measurement

The field emission tests are performed on a diode structure, in which CNTWNCCs are separated from the anode, indium-tin-oxide (ITO) glass, using 500 μm glass as spacers. Green color phosphor coated ITO is used to probe the emission image and the emission density. The emission current (I) is measured as a function of the anode-to-cathode voltage in a vacuum of 1×10^{-6} torr. The Fowler-Nordheim theory [12] is the most commonly used model for the emission of cold electrons from a metal under a strong applied field. Figures 9.5 (a) and (b) displays the I-V curve and F-N plot of CNTWNCCs. Plotting Ln (I/V^2) against 1/V (F-N plot) should yield a straight line, implying that CNTWNCCs exhibit the property of field emission. A useful parameter for comparison with other field emitters is E_{to} (turn-on field), which is the field V/d (applied voltage/ distance between cathode and anode) required to produce a current of 10 $\mu A/cm^2$. The current density, which is 100 $\mu A/cm^2$ as a function of time is further measured to determine the stability of the emitters. Experimental data reveal a fluctuation is less than 10 % in one hour. The I-V results clearly show that CNTWNCCs exhibit a favorable field emission property, that is, a turn-on field of 1.38 V/μm and 565 $\mu A/cm^2$ at 2.2 V/μm. It is attributed to the following reasons (I) good alignment and (II) high aspect ratio. Besides, nanocrystalline chromium carbides are also expected to be the improvement in the

field emission property. Due to the nanosize effect, the nanoparticles may offer higher

electron-supply capability as well as better surface electrical conductivity of the

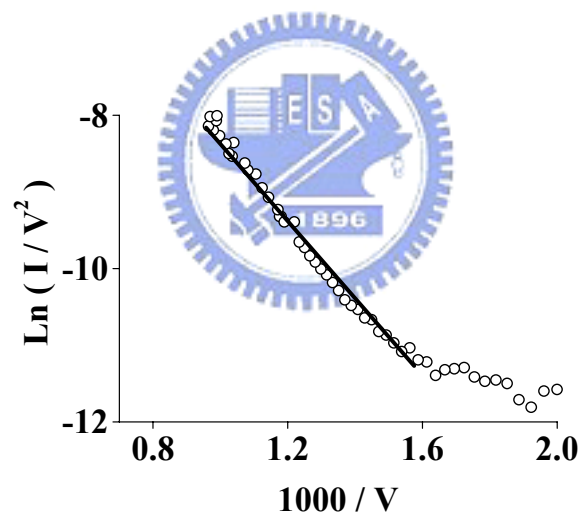CNTWNCCs as compared to those pure carbon nanotips.

(a)
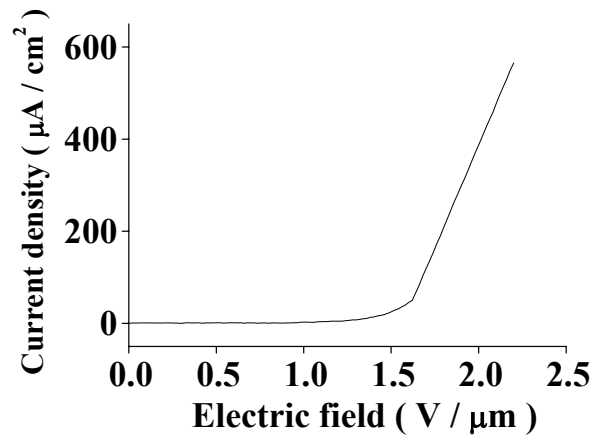
(b)

Fig. 9.5 (a) The current density (J) versus electric field (E) and (b) F-N plot of

CNTWNCCs.

9.4. Conclusion

In this chapter, the nanocrystalline chromium carbides are self-embedded on the pure carbon nanotips. Some major results are summarized as follows:

1. Due to the H_2 plasma etching effect, Cr films become activate and nanoparticles, offering a confined space in which nanoscience can be conducted.

2. Based on SEM pictures, CNTWNCCs grow up to about 1 μm long and 60 nm in diameter, causing them to exhibit a high aspect ratio, and making them good candidates for the application of field emission.

3. The alignment of CNTWNCCs is primarily resulted from plasma-induced effect. This suggests that the CNTWNCCs orientation is influenced by the electrical field established on the immersed substrate surface in the plasma.

4. As growing carbon nanotips, the weak force between Cr and substrate causees Cr nanoparticles to gradually lift off and to carburize into chromium carbides. This growth mechanism is analogous to the tip-growth model of carbon nanotubes.

5. CNTWNCCs perform well in field emission property because of (I) good alignment; (II) high aspect ratio and (III) nanosize effect of chromium carbides.

9.5 Reference

1. S.Iijima, Nature (London) 354,56 (1991).

2. H.Dai, J.H.Hafner, A.G.Rinzler, D.T.Colbert and R.E.Smally, Nature (London) 384, 147 (1996).

3. P.G.Collins and A. Zettl, Appl. Phys. Lett. 69, 1969 (1996).

4. H.Schmid and H.W.Fink, Appl. Phys. Lett. 70, 2679 (1997).

5. Q.H.Wang, T.D.Corrigan, J.Y.Dai, R.P.H.Chang and A.R.Krauss, Appl. Phys. Lett. 70, 3308 (1997).

6. Y. Tu, Z. P. Huang, D. Z. Wang, J. G. Wen, and Z. F. Ren, Appl. Phys. Lett. 80, 4018 (2002).

7. Anyuan Cao, Bingqing Wei, Y. Jung, Robert Vajtai, P. M. Ajayan, and G. Ramanath, Appl. Phys. Lett. 81, 1297 (2002).

8. Y. Avigal and R. Kalish, Appl. Phys. Lett. 78, 2291 (2001).

9. C. L. Tsai, C. F. Chen, and L. K. Wu, Appl. Phys. Lett. 81, 721 (2002).

10. Jaehee Han, Ji-Beom Yoo and Chong Yun Park. J.Appl.Phys. 91, 483 (2002).

11. F. Okuyama, T. Hayashi, and Y. Fujimoto, J. Appl. Phys. 84, 1626 (1998).

12. R. H. Fowler and L. W. Nordheim. Proc. Royal. Soc. London A. 119, 173 (1928).